Comparison of chloride-induce corrosion of steel in cement and alkali-activated fly ash mortars

Antonino Runci[1] and Marijana Serdar[1]

[1] University of Zagreb, Faculty of Civil Engineering, Department of Materials, Croatia
marijana.serdar@grad.unizg.hr

Abstract. The aim of this paper is to make an initial evaluation of chloride-induced corrosion behaviour of steel in alkali-activated fly ash and compare it to behaviour of classical cement mortar. Fly ash used in this research was obtained from regional production and was activated with sodium silicate and sodium hydroxide. Setup for evaluating corrosion behaviour consisted of structural steel plate covered with mortar layer under tap water or simulated seawater solutions. Corrosion behaviour of structural steel plates was monitored by Open Circuit Potential (OCP) and Linear Polarization (LP). The mortars have been additionally characterized by their mechanical properties, pore structure obtained by mercury intrusion porosimetry (MIP), electrical resistivity and chloride migration according to NT BUILD 492.

Keywords: alkali-activated fly ash, corrosion, chloride, linear polarisation, chloride diffusion, migration.

1 Introduction

Alkali-activated materials (AAMs) are alternative type of binder based on an alkali activator and an aluminosilicate powder, which is generally a by-product of other industrial activities [1]. AAMs are recently finding high interest due to the enormous demands for production of concrete, especially in developing countries, and the urgent need for a reduction of CO_2 emissions in industrial activities. According to McLellan et al. [2] AAMs can save in term of greenhouse gas emission around 44-64% in Australia, coming mostly from activators production and transportation and pretreatment of precursors.

Despite different studies indicating good performance of AAMs, there are still not enough studies in the literature about long-term durability performance related to chloride ingress and corrosion of embedded steel. The knowledge available on corrosion of steel in ordinary Portland cement cannot be directly transferred to AAMs, due to their significantly different chemical and physical properties. Furthermore, AAMs have displayed wide variability due to the changeable chemical and physical properties of by-products used and types and ratios of activators, which makes any generalization about these systems practically impossible.

The corrosion of steel embedded in concrete is the first cause of degradation and poor durability in reinforced concrete (~70-90% of times) [3]. The cause of embedded steel corrosion is the breakdown of the protective passive layer at the steel-concrete interface formed at high pH. The carbonation process and/or chloride ingress drive the activation of steel surface lowering the pH and the precipitation of corrosion product at the interface [4].

This paper presents results of a study on durability of alkali-activated mortar based on fly ash compared to the OPC. The aim of the study was to evaluate the applicability of this systems in aggressive environment and characterize the diffusion and microstructural behavior.

2 Experimental program

2.1 Materials and Mix design

The alkali-activated formulation (labelled hereafter FA) used was based on fly ash class F coming from Elektroprivreda BiH, TE Kakanj, Bosnia & Hercegovina. The formulation was adopted from RILEM TC 247-DTA round robin test studies [5]. In present study, fly ash was activated with sodium silicate Geosil 34417 from Woellner with Ms = 1.68 and NaOH solution. The aggregate was local limestone sand with granulometry of 0-4 mm. The binder/aggregate used for FA mix was 0.375. FA was mixed with 16.5 sodium silicate/fly ash ratio and 5.9 NaOH/fly ash ratio. The reference mortar mix (labelled hereafter OPC) was prepared with CEM I from CEMEX, Croatia and with a water/binder ratio 0.5. **Table 1** shows the chemical composition of fly ash and OPC.

Table 1. Chemical composition of used materials.

	CaO	SiO_2	Al_2O	Fe_2O	MgO	K_2O	Na_2O	SO_3
Fly ash	13.04	51.10	20.58	5.39	2.15	1.99	0.89	1.72
OPC	64.04	19.32	4.86	2.94	1.83	0.82	0.23	2.75

Mortar samples of OPC were prepared according to EN 196-1. FA mortar was prepared using following procedure: dry powders and aggregate were mixed for a minute, and then again for 6 minutes adding continuously activators; the mixing was paused for a minute and then again mixture was mixed for additional minute. Samples were demolded after one day and were then tightly wrapped to prevent moisture loss for continued sealed curing until testing.

2.2 Methods

The compressive strength of mortar specimens was determined on prisms 4x4x16 cm according to EN 196-1 with a loading rate of 2400 kN for compressive strength at 28 days of curing. Mercury Intrusion porosimetry (MIP) was used to provide information

regarding the pore size distribution and pore volume of the mortars [6]. Specimens for MIP were immersed in isopropanol for 14 days and then vacuum dried. Autopore IV 9510 was used for MIP measurement and the pore size ranging from 350 to 0.007 μm were detected.

To detect the alkaline condition of mortar the pH was measured per each specimen every 7 days. From each testing 5 g of mortar powder was collected and mixed with 5 ml dis-tilled water for 24h at room temperature. pH of the obtained leachate solution was deemed to be an acceptable approximation of the pH of the mortar pore electrolyte [7].

The non-steady-state chloride migration was conducted according to NT Build 492. Three specimens per mix with 100 mm diameter and 50 mm height were tested after 28 days of curing. $AgNO_3$ colorimetric analysis was applied at the end of the test. Chloride penetration was measured as the visible boundary between white precipitation of AgCl when chloride is present in sufficient quantities and precipitation of brown Ag_2O otherwise. An important parameter for this test is the chloride concentration at which the colour changes (c_d). The NT BUILD 492 recommends the value of 0.07 N for cd for OPC concrete. However, for alkali-activated fly ash c_d = 0.21 was applied [8], [9] to take into account hydroxide ions (pH value).

The monitoring of the corrosion of steel in mortar was carried out using an unconventional three-electrode cell suggested by Šoić et al. [10] with a PAR VMP2 potenciostat/galvanostat. The samples were prepared using carbon steel plate as working electrodes, which simulated the reinforcement inside the concrete. Carbon steel plates were polished until even metallic surface was obtained. On top of the steel plate, a polymeric cylinder was glued with silicon. This cylinder was used as a mold for the prepared mortar. A graphite stick was placed inside the solution to act as the counter electrode, and saturated calomel electrode (SCE) was positioned to act as the reference electrode (Figure 1).

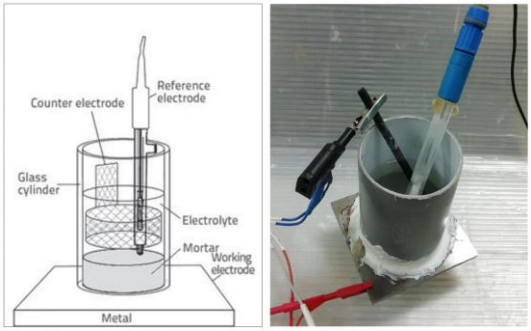

Fig 1. Three-electrode electrochemical cell with steel plate as working, graphite stick as counter and saturated calomel as reference electrode.

Samples were cured for 7 days, after which 0.130 ml of tap water for the reference specimens and 0.130 ml of 3.5 % NaCl were added to each cell (3 per mixes). Sam-

ples were covered with plastic foil to prevent electrolyte evaporation in the period between measurements. Open-circuit potential (OCP) and linear polarization resistance (LPR) were performed approximately every 7 days, respectively for 15 and 1 minutes. For LPR measurements, the steels were polarized to ±10 mV of corrosion potential (E_{corr}) at a scan rate of 0.166 mV/s. The polarisation resistance (R_p) was calculated using the modified Stern-Geary equations. Corrosion current densities were calculated from the measured R_p values, using theoretical value of Tafel constant B = 52 mV.

3 Results and discussion

Table 2 displays slump and strength results for OPC and FA after 28 days of humidity chamber curing for OPC and sealed curing for FA. Despite the higher slump value, FA mix was sticky and less workable due to the high activator content. FA mix showed higher compressive strength than OPC mix. FA mix also showed better performance than average value from RILEM TC 247 [5].

Table 2. Consistency and compressive strength for FA and OPC mix.

	Consistency by slump (mm)	Compressive strength (MPa)
OPC	160	59.48
FA	175	77.38

The pH is the main factor influencing the stability of passive film on steel. Figure 2 shows the pH values of OPC and FA mixes at 7, 14, 21 and 28 days of curing compared with resistivity values.

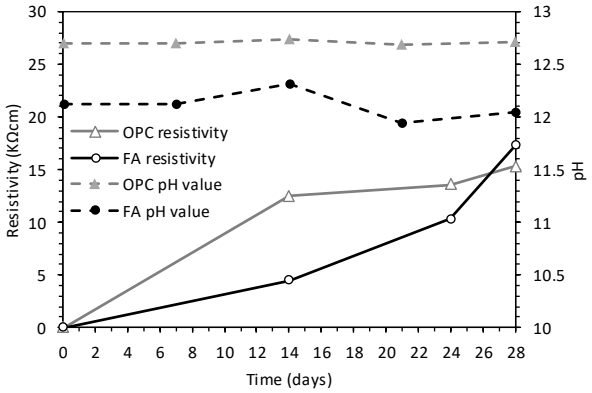

Fig. 2. Evolution of resistivity (full line) and pH (dotted line) of FA and OPC mix.

OPC data were almost stable throughout the testing period. However, values for FA mix showed a slow reduction from 12.12 until 12.04. Monticelli et al. [11] showed

that pH of OPC has higher stability after 11 weeks of wet-dry cycles rather than FA mortars. The difference between the two systems could be attributed to an early carbonation of alkali-activated mix, which was earlier reported in the literature [12]. The resistivity of mortars was increasing with the time. After 14 days, OPC stabilized, while FA values sharply increased at 28 days.

Compared to OPC, FA showed a drastically higher resistance to migration under a forced chloride penetration. van Deventer et al. [13] demonstrate a congruent behavior with alkali-activated slag and slag-fly ash systems [9]. The high resistivity and the low migration are probably connected to the lower porosity (Figure 3) of FA systems that reduce the diffusion through the pores [14].

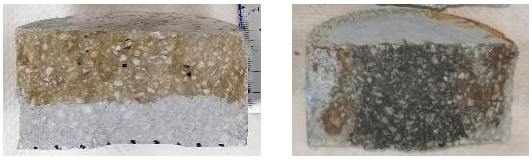

$D = 14 \times 10^{-12}$ m^2/s $D = 3 \times 10^{-12}$ m^2/s

Fig. 3. Colorimetric analysis with $AgNO_3$ on specimen of OPC and FA mix after chloride migration testing according to NT BUILD 492.

In OPC, there are two peaks in the differential curve (Figure 4), correspondig to two pore systems: gel pores and capillary pores. The gel pores are formed within the formation of the CSH gels; their pore size diameter ranges is from 0.5 nm to 0.01 μm. The capillary pores refer to the space left by the water which did not react during the hydration reaction; the capillary pore sizes range from 0.01 μm to10 μm.

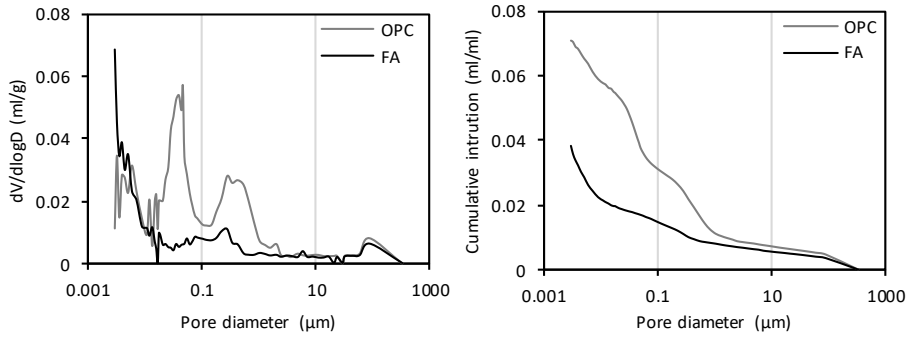

Fig. 4. Pore size distribution for OPC and FA mix obtained by MIP.

Similarly, FA shows two peaks (Figure 4): the first peak reflecting pore sizes with diameter in the range of several nm to 0.04 μm, corresponding to the gel pore; and a second peak corresponding to pore size ranges of 0.1–1 μm, representing the 'capillary pores' [15]. Differently than the paste from Ma et al. [16], FA mortar shows at the same condition a lower total porosity than OPC. The highest gel porosity of FA is probably an overstimation due an 'ink-bottle' effect. This effect is due to the

cavities left by fly ash particles dissolution and have dimension to the capillarity pores. These pores differnce form OPC capillaritry pores because they do not show a continous network; rather, they are connected to extern with fines pores network [17].

Corrosion potential (E_{corr}) is the most common corrosion index, it is only a qualitative parameter and does not necessarily correlate with corrosion corrent density (i_{corr}), which describes the rate of dissolution of steel. Figures 5 shows the trend of the elctrochemical parameters in reference and corrosion enveronment. The more negative potential value (E_{corr}) for FA is not necessarily indicative of a higher risk of corrosion, but it may be consequence of several factors: the lower pH value of FA (as seen on Figure 2) and the finer porosity which decreases the permeability of oxygen in cathodic areas which leads to more negative corrosion potential values (as seen on Figure 3) [18], [19].

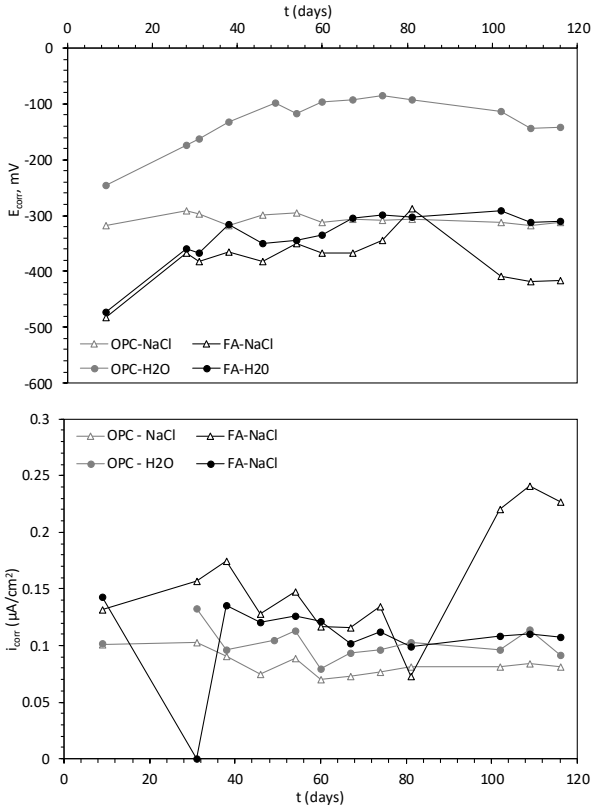

Fig. 5. Corrosion potential and current of steel in OPC and FA mortar exposed to tap water and to 3.5% NaCl solution.

The corrosion current density (i_{corr}) of steel in FA was higher than steel in OPC, although the difference is not as significant. The deviation of FA in corrosion environment indicates the initiation stage of corrosion. Despite the observation of lower porosity in alkali-activated fly ash compared to OPC, confirmed also by a lower chloride migration coefficient and higher resistivity (as seen on Figure 2 and 3), the

electrochemical measurement shows an initial corrosion after 100 days of measurement. This behavior may be influenced by the microstructure evolution of FA. Ma et al. [16] demonstrated through MIP measurement that the capillaries pores in alkali-activated fly ash still exist after several months of curing; rather in OPC the hydration products continuously fill the cavities till vanishing the peak corresponding to the capillary pores. However, to further investigate this hypothesis, additional measurements should be performed.

4 Conclusion

This study showed comparison between OPC and alkali-activated fly ash mortar under chloride environment. Alkali-activated fly ash showed higher compressive strength, significantly lower chloride migration coefficient and electrical resistivity. Improved properties of FA mix compared to OPC mix can be attributed to finer pore size distribution, as evident form MIP presented in the paper. However, regardless of this lower chloride migration coefficient and finer pore size distribution, corrosion did occur in FA system sooner than in the OPC system. Reasons for sooner corrosion initiation in this specific system are focus of current research.

Acknowledge

Research presented in this paper was performed within project DuRSAAM, which has received funding from the European Union's Horizon 2020 research and innovation programme under grant agreement No 813596. Research is also supported by the project "Alternative Binders for Concrete: understanding microstructure to predict durability, ABC", funded by the Croatian Science Foundation under number UIP-05-2017.

References

[1] J. Provis, and J. van Deventer, "Alkali Activated Materials: State-of-the-Art Report, RILEM TC 224-AAM" *Springer, Dordrecht*, vol. 13, 2014.

[2] B. C. Mclellan, R. P. Williams, J. Lay, A. Van Riessen, and G. D. Corder, "Costs and carbon emissions for geopolymer pastes in comparison to ordinary portland cement," *Journal of Cleaner Production*, vol. 19, no. 9–10, pp. 1080–1090, 2011.

[3] U. M. Angst, "Challenges and opportunities in corrosion of steel in concrete," *Materials and Structures/Materiaux et Constructions*, vol. 51, no. 1, pp. 1–20, 2018.

[4] S. Ahmad, "Reinforcement corrosion in concrete structures, its monitoring and service life prediction - A review," *Cement and Concrete Composites*, vol. 25, no. 4-5 SPEC, pp. 459–471, 2003.

[5] J. L. Provis *et al.*, "RILEM TC 247-DTA round robin test: mix design and reproducibility of compressive strength of alkali-activated concretes,"

Materials and Structures, vol. 52, no. 5, pp. 1–13, 2019.

[6] K. Scrivener, R. Snellings, and B. Lothenbach, A Practical Guide to Microstructural Analysis of Cementitious Materials. 2015.

[7] V. Räsänen and V. Penttala, "The pH measurement of concrete and smoothing mortar using a concrete powder suspension," Cement and Concrete Research, vol. 34, no. 5, pp. 813–820, 2004.

[8] A. Noushini, A. Castel, J. Aldred, and A. Rawal, "Chloride diffusion resistance and chloride binding capacity of fly ash-based geopolymer concrete," *Cement and Concrete Composites*, no. May 2018, p. 103290, 2019.

[9] I. Ismail *et al.*, "Influence of fly ash on the water and chloride permeability of alkali-activated slag mortars and concretes," *Construction and Building Materials*, vol. 48, pp. 1187–1201, 2013.

[10] I. Šoić, S. Martinez, I. Lipošćak, and B. Mikšić, "Development of method for assessing efficiency of organic corrosion inhibitors in concrete reinforcement," *Gradjevinar*, vol. 70, no. 5, pp. 369–375, 2018.

[11] C. Monticelli *et al.*, "A study on the corrosion of reinforcing bars in alkali-activated fly ash mortars under wet and dry exposures to chloride solutions," *Cement and Concrete Research*, vol. 87, pp. 53–63, 2016.

[12] M. Fernández Bertos, S. J. R. Simons, C. D. Hills, and P. J. Carey, "A review of accelerated carbonation technology in the treatment of cement-based materials and sequestration of CO2.," *Journal of hazardous materials*, vol. 112, no. 3, pp. 193–205, 2004.

[13] J. S. J. Van Deventer *et al.*, "Microstructure and durability of alkali-activated materials as key parameters for standardization," *Journal of Sustainable Cement-Based Materials*, vol. 4, no. 2, pp. 120–134, 2015.

[14] J. L. Provis, R. J. Myers, C. E. White, V. Rose, and J. S. J. Van Deventer, "X-ray microtomography shows pore structure and tortuosity in alkali-activated binders," *Cement and Concrete Research*, vol. 42, no. 6, pp. 855–864, 2012.

[15] J. Zhou, G. Ye, and K. van Breugel, "Characterization of pore structure in cement-based materials using pressurization-depressurization cycling mercury intrusion porosimetry (PDC-MIP)," *Cement and Concrete Research*, vol. 40, no. 7, pp. 1120–1128, 2010.

[16] Y. Ma, J. Hu, and G. Ye, "The pore structure and permeability of alkali activated fly ash," *Fuel*, vol. 104, pp. 771–780, 2013.

[18] D. M. Bastidas, A. Fernández-Jiménez, A. Palomo, and J. A. González, "A study on the passive state stability of steel embedded in activated fly ash mortars," *Corrosion Science*, vol. 50, no. 4, pp. 1058–1065, 2008.

[19] M. Babaee, M. S. H. Khan, and A. Castel, "Passivity of embedded reinforcement in carbonated low-calcium fly ash-based geopolymer concrete," *Cement and Concrete Composites*, vol. 85, pp. 32–43, 2018.